International Journal of Pharmaceutics: X 4 (2022) 100123

Contents lists available at ScienceDirect

International Journal of Pharmaceutics: X

journal homepage: www.sciencedirect.com/journal/international-journal-of-pharmaceutics-x

Characterization of radicals in polysorbate 80 using electron paramagnetic resonance (EPR) spectroscopy and spin trapping

Judith J. Mittag [a,1], Marie-Luise Trutschel [b,1], Helen Kruschwitz [b], Karsten Mäder [b], Julia Buske [a], Patrick Garidel [a,*]

[a] Boehringer Ingelheim Pharma GmbH & Co. KG, Innovation Unit, PDB-TIP, Birkendorfer Straße 65, 88397 Biberach an der Riss, Germany
[b] Martin-Luther-University Halle-Wittenberg, Institute of Pharmacy, Faculty of Biosciences, Wolfgang-Langenbeck-Strasse 4, 06120 Halle (Saale), Germany

ARTICLE INFO

Keywords:
EPR
Polysorbate
Radical
Oxidation
Peroxide
Spin trap
DMPO

ABSTRACT

Polysorbates are an important class of nonionic surfactants that are widely used to stabilize biopharmaceuticals. The degradation of polysorbate 20 and 80 and the related particle formation in biologics are heavily discussed in the pharmaceutical community. Although a lot of experimental effort was spent in the detailed study of potential degradation pathways, the underlying mechanisms are only sparsely understood. Besides enzymatic hydrolysis, another proposed mechanism is associated with radical-induced (auto)oxidation of polysorbates. To characterize the types and the origin of the involved radicals and their propagation in bulk material as well as in diluted polysorbate 80 solutions, we applied electron paramagnetic resonance (EPR) spectroscopy using a spin trapping approach. The prerequisite for a meaningful experiment using spin traps is an understanding of the trapping rate, which is an interplay of (i) the presence of the spin trap at the scene of action, (ii) the specific reactivity of the selected spin trap with a certain radical as well as (iii) the stability of the formed spin adducts (a slow decay rate). We discuss whether and to which extent these criteria are fulfilled regarding the identification of different radical classes that might be involved in polysorbate oxidative degradation processes. The ratio of different radicals for different scenarios was determined for various polysorbate 80 quality grades in bulk material and in aqueous solution, showing differences in the ratio of present radicals. Possible correlations between the radical content and product parameters such as the quality grade, the manufacturing date, the manufacturer, the initial peroxide content according to the certificate of analysis of polysorbate 80 are discussed.

1. Introduction

Polysorbate 20 and 80 (PS) are surfactants that are widely used in pharmaceutical formulations, especially biopharmaceuticals, to protect proteins from e.g. damage during transport and storage. Therefore, it is necessary to evaluate the functionality of nonionic surfactants and maintain a certain level of intact surfactant in solution during the complete shelf-life of a drug product (Ravuri, 2018), to prevent protein degradation (Larson et al., 2020a; Kranz et al., 2019; Zhang et al., 2017). There is a growing number of biopharmaceuticals formulated with PS entering the market. Hence, understanding which factors influence PS stability in formulations has moved into the focus of research activities within the last years (Larson et al., 2020a; Kranz et al., 2019; Zhang et al., 2017), but was already under discussion in the past (Donbrow et al., 1978; Bates et al., 1973; Jaeger et al., 1994). For a comprehensive introduction to this extensive topic, we refer to Kishore et al. (2011) and Dwivedi et al. (2018) (Kishore et al., 2011a; Kishore et al., 2011b; Dwivedi et al., 2018). PS consists of a hydrophilic sorbitan head group with four chains of polyoxyethylene (POE) of which one to four are esterified with lipophilic fatty acids (FAs) ranging from caproic (6:0) to linoleic acid (18:2) (Ravuri, 2018; Evers et al., 2021) (Table S1). Both polysorbates, PS20 and PS80, are highly complex and heterogeneous mixtures of hundreds of single compounds consisting of mono- to tetraesters (Larson et al., 2020a; Dahotre et al., 2018). The type and ratio of

Abbreviations: alkyl radical, $R^{\bullet}$; alkoxyl radical, $RO^{\bullet}$; china grade, CG; certificate of analysis, CoA; 5,5-dimethyl-1-pyrroline-N-oxide, DMPO; electron paramagnetic resonance, EPR; fatty acid, FA; hydrogen peroxide, H_2O_2; high purity, HP; hydroxyl radical, $HO^{\bullet}$; hydroperoxide, ROOH; peroxyl radical, $ROO^{\bullet}$; polyoxyethylene, POE; polysorbate, PS; all-oleate, AO; reactive oxygen species, ROS; superoxide, $O_2^{\bullet-}$; super-refined, SR.

* Corresponding author.
E-mail address: Patrick.Garidel@boehringer-ingelheim.com (P. Garidel).

[1] Shared first authorship.

https://doi.org/10.1016/j.ijpx.2022.100123
Received 20 June 2022; Accepted 21 June 2022
Available online 23 June 2022

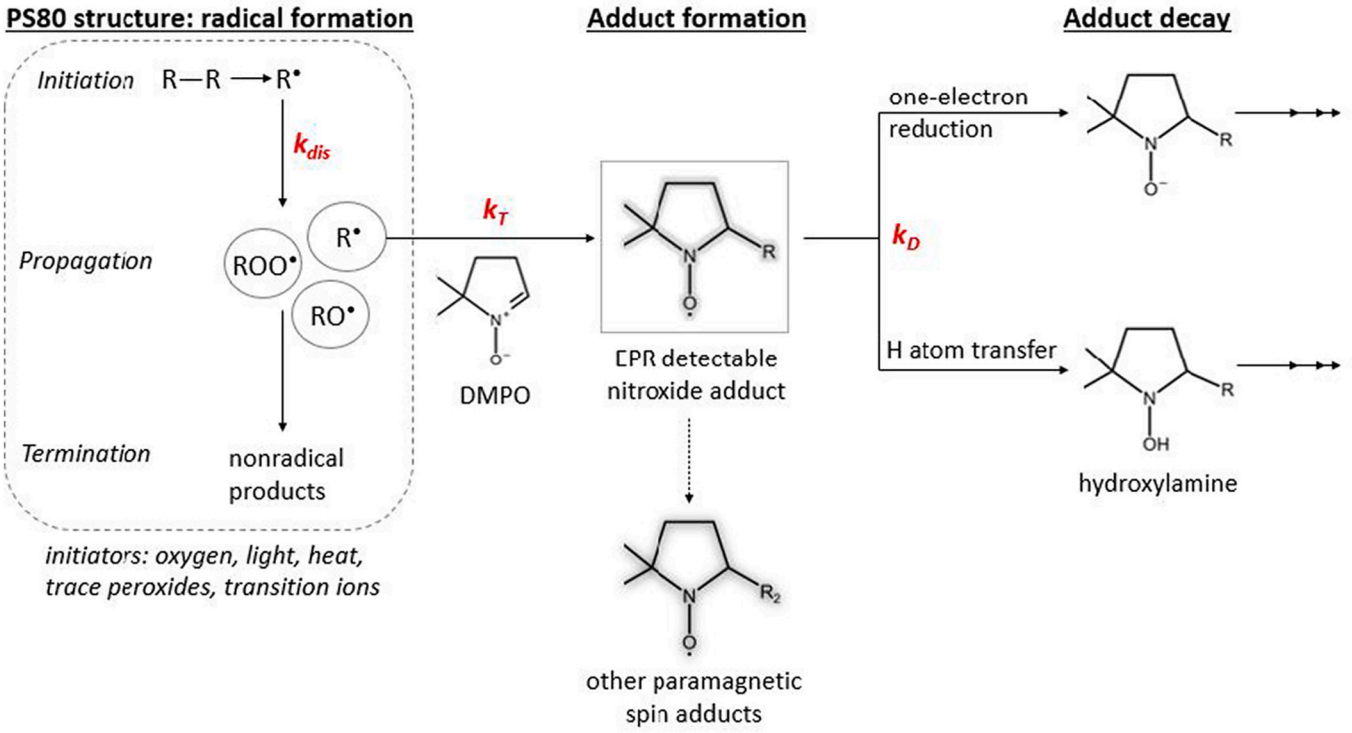

Scheme 1. Schematic representation of the radical chain reaction mechanism (left), EPR detectable spin adducts of DMPO (5,5-Dimethyl-1-Pyrroline-N-Oxide) (middle), and two possible adduct decay mechanisms (right). The rate constants controlling the different processes are highlighted in red. The rate constants vary depending on the radicals and their environment.

the fatty acids define the specific kind of PS, e.g. for PS20, the main fatty acid present is lauric acid (12:0), while for PS80 it is oleic acid (18:1). The pharmacopeias (Ph. Eur., USP, JP, ChP) define acceptable ranges for the different FAs and other parameters such as the peroxide value for PS (Dwivedi et al., 2018). A certain amount of free fatty acids (FAs) is already present in commercially available PS raw material (Larson et al., 2020a), due to the manufacturing of polysorbate, as well as traces of peroxides. Peroxides are products of radical reactions, but also the source and initiators for further radical reactions. Therefore, the peroxide value is the first indicator for the propensity of radicals being present in a PS sample as described in more detail below.

The requirements for PS80 are harmonized between the European, Japanese, and United States Pharmacopeias, in which a fraction of >58% of the esterified FAs is demanded to be oleic acid. A much lower percentage of palmitic, myristic, stearic, linoleic, and linolenic acid esters are present as well, but are not necessarily obligatory ("smaller than" definition in pharmacopeias). Within these limits, "more purer quality" grades aside from established ones like high purity (HP) became available. Apart from super-refined (SR) qualities that fulfill the ChP requirements for injectables for PS80 from 2015 with a minimal oleic acid content of 98%, like all-oleate (AO) and china grade (CG), are available (Grabarek et al., 2020). In this context "pure" refers to an increased amount of the PS type defining FA and low fractions of other FAs. In the case of PS80, this relates to a fraction of oleic acid (18:1) for CG and AO of larger than 99% compared to about 87% for SR and 75% for HP qualities. An overview of the different composition features of these quality grades can be found in Knoch et al. (Knoch et al., 2021), Yang et al.[15,] (Yang et al., 2021) and Table S1. The heterogeneity of commercially available PS seems to be a double-edged matter. On one hand, although little is known about the functionality of specific isolated PS fractions, this variety might be the key to the beneficial and stabilizing properties of PS. On the other hand, the heterogeneity leads to different susceptibilities to degradation of the individual components during storage in pharmaceutical formulations (Grabarek et al., 2020; Khan et al., 2015; Rabe et al., 2020; Nayem et al., 2020).

Despite comprehensive studies, the exact details of degradation pathways have not been understood yet and efforts are ongoing to develop adequate analytical characterization methods (Penfield and Rumbelow, 2020; Borisov et al., 2015; Evers et al., 2020; Puschmann et al., 2019). Generally, hydrolysis and oxidation are discussed as the two main degradation pathways for PS. A hallmark of hydrolysis – especially of enzymatic one – is the formation of free FAs as a degradation product (Kishore et al., 2011a; Kishore et al., 2011b; Dwivedi et al., 2018). As shown in different studies, the released free fatty acids can cluster into visible particles and thereby compromise the drug product quality (Dixit et al., 2016; Labrenz, 2014; Tomlinson et al., 2015). Hydrolysis, especially enzymatically driven, is linked to the presence of remaining host cell proteins, such as esterases and lipases (Labrenz, 2014; Graf et al., 2021; Zhang et al., 2021; Glücklich et al., 2021). Additionally, chemical hydrolysis driven by pH is possible but highly unlikely in the considered pharmaceutical relevant pH range from 5 to 7 (Dwivedi et al., 2020).

Here, we focus on degradation caused by (auto)oxidation in the context of radical chain reactions as proposed by Larson et al. (2020) or Yao et al. (2009) (Larson et al., 2020b; Yao et al., 2009). An indicator for oxidation is the diversity of final and intermediate degradation products such as peroxides, aldehydes, alkanes, and a small number of short-chain acids, such as acetic or formic acid (Kishore et al., 2011a; Kishore et al., 2011b; Dwivedi et al., 2018). This variety of degradation products has its origin in the numerous targets of underlying degradation processes. Oxidation can occur at the POE units, but also at the site of double bonds of FAs such as oleic acid (18:1) or other unsaturated FAs (Zhang et al., 2017; Dahotre et al., 2018). A higher degree of unsaturation favors oxidative degradation.

Reactive species such as peroxides can initiate the chain reaction but are as well intermediates during oxidation promoting the reaction. The pharmacopeias allow a peroxide value for PS80 of <10 (mEq O_2)·kg^{-1} determined by compendial methods (EU70035A and EU70035B). The certificates of analysis (CoAs) show that this value is usually much lower (< 1 (mEq O_2)·kg^{-1}, Table S1).

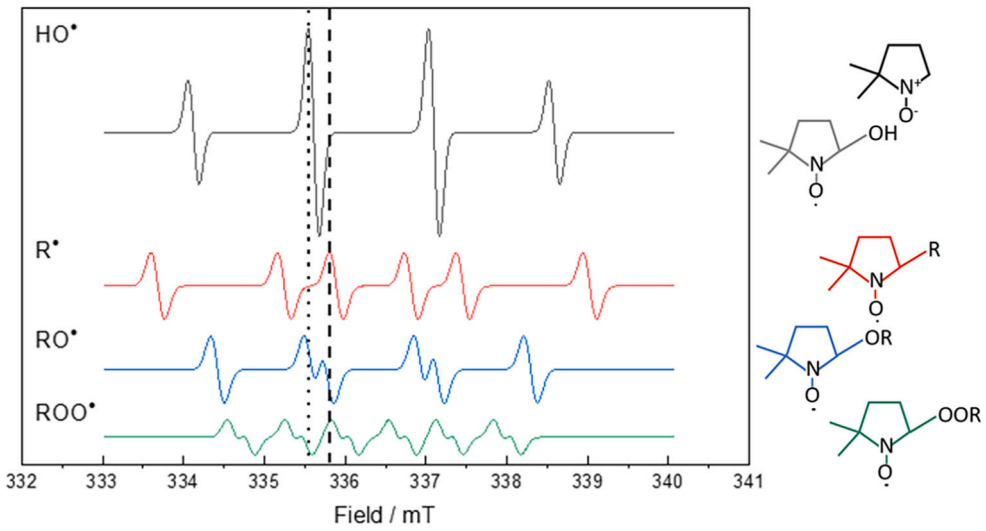

Fig. 1. Electron paramagnetic resonance (EPR) patterns of the different radical species (left) determined by simulation with the corresponding spin adducts of DMPO (5,5-Dimethyl-1-Pyrroline-N-Oxide) (right). The dotted and dashed lines correspond to the signal that was tracked during spin kinetics evaluation.

Hydrogen peroxide (H_2O_2) is not a radical by nature, but it can form hydroxyl radicals ($HO^\bullet$) via several pathways. In addition to photocatalytic decomposition, H_2O_2 can react with transition metal ions such as Fe^{2+} via the Fenton reaction (Eq. (1)) or with superoxide ions ($O_2^{\bullet-}$) via the Haber-Weiss reaction (Eq. (2)) (Phaniendra et al., 2015).

$$Fe^{2+} + H_2O_2 \rightarrow Fe^{3+} + HO^\bullet + OH^- \quad \text{(Fenton reaction)} \tag{1}$$

$$O_2^{\bullet-} + H_2O_2 \rightarrow O_2 + HO^\bullet + OH^- \quad \text{(Haber} - \text{Weiss reaction)} \tag{2}$$

Therefore, even tiny amounts of peroxides either from the manufacturing processes of PS or the drug substance (protein) might cause significant effects after reacting with impurities of redox-active metal ions (e.g. Fe^{2+}/Fe^{3+}, Cu^{2+}or Cu^{+}) (Kishore et al., 2011a). Consequently, the presence of peroxides can be detrimental not only to the stability of PS itself but also to the therapeutic protein, which can be degraded as well.

(Auto)oxidation of PSs can be described by a free radical chain reaction, where radicals act as an oxidizing agent removing electrons from e.g. polyunsaturated fatty acids or POEs.

The mechanism is divided into three phases: initiation, propagation, and termination (Donbrow et al., 1978; Kerwin, 2008) (Scheme 1). In the initiation phase, an alkyl radical ($R^\bullet$) is formed by the abstraction of an H-atom from e.g. a methylene (RH) unit. This process can be triggered via various factors such as exposure to light, temperature, reactive oxygen species (ROS), and/or impurities such as trace metals. ROS are defined as highly reactive chemicals formed from O_2 including free radicals ($HO^\bullet$, $O_2^{\bullet-}$, $HOO^\bullet$), but also H_2O_2, hydroperoxide (ROOH), or singlet oxygen ($^1O_2$). During the propagation phase, $R^\bullet$ reacts with oxygen to a peroxyl radical ($ROO^\bullet$). The peroxyl radicals further react to $R^\bullet$ and ROOH which can then propagate the radical chain reaction. Formed ROOHs include lipid hydroperoxides such as (*Z*)-8-hydroperoxy-9-enoic and (*E*)-10-hydroperoxy-8-enoic products for oleic acid (Yin et al., 2011). As long as the radical reacts with nonradicals, it always generates another radical. During the termination phase, the radical content decreases as two radicals form a nonradical product such as aldehyde (e.g. formaldehyde or acetaldehyde). The aldehydes originating from polysorbate degradation are suspected to be contact allergens and can react with protein to reactive carbonyl adducts (Bergh et al., 1998; Moghaddam et al., 2011).

The radical reaction can be terminated when all oxidants are consumed, or antioxidants are used to stop the chain reaction. Since the radical content increases first and then decreases again when the reaction enters the termination phase, it is difficult – if not impossible – to assess whether a sample is currently in the initiation or the termination phase without a reference. Apart from the peroxide value in the CoA, no further information regarding the initial radical content is available from the manufacturer. Therefore, a reference measurement is always required, since both phases could result in similar total radical content, but maybe with varying radical ratios. However, the latter is still under debate. In this study, we focus on the analysis of radicals in PS80 due to its, described, higher propensity for oxidative degradation by oxidation caused by the higher content of unsaturated FAs in comparison to PS20 (Kishore et al., 2011b; Yao et al., 2009) and monitor whether the radical species may vary.

Only a few analytical approaches are capable of radical detection. Besides the characterization of the products of the radical reaction by mass spectrometry (Penfield and Rumbelow, 2020; Borisov et al., 2015; Evers et al., 2020; Puschmann et al., 2019), also fluorescent assays are available such as the ferrous oxidation-xylenol orange (Fox) assay or Amplex Red assay (Jiang et al., 1992; Deiana et al., 2009; Wolff, 1994). They are popular due to their straightforward handling and their potential for high-throughput applications. Their important shortcoming is that they lack the specificity and potential to differentiate various types of radicals from each other. EPR (electron paramagnetic resonance, also known as ESR, electron spin resonance) spectroscopy provides an alternative approach to solve radical related research questions. EPR is a spectroscopic method that is capable to determine the presence of free radicals in solution and the solid-state (Samouilov et al., 2004) due to their paramagnetic properties. It can be used to identify and quantify these radical species. Samples with a permanent magnetic moment (unpaired electrons) such as free radicals split into their degenerated energy levels after applying an external magnetic field. Microwave radiation matching the energy gap between the levels can be absorbed (Lardinois et al., 2008). Most materials are EPR silent and do not contain sufficient concentrations of radical species. However, EPR active molecules (e.g. spin probes and spin labels) can be used to monitor the microenvironment in drug delivery systems and to measure the microviscosity, -polarity or -acidity (Kempe et al., 2010). The spin trapping technology can be used to detect short-lived radical species after their reaction with a spin trap (Janzen, 1995; Buettner and Mason, 1990) (see Scheme 1 and Fig. 1). The spectra allow us to draw conclusions on the radicals present in the solution. Each radical species has its own characteristic EPR peak pattern, allowing its identification (Villamena, 2017). For instance, $HO^\bullet$ possesses a prominent four-peak pattern (see

Fig. 1, top). If more than one radical species is present in the solution, their individual patterns superimpose and analysis becomes more challenging and complex. Nevertheless, a simulation-fitting approach can be used to determine the ratios of the different radicals (Etienne et al., 2017).

Although EPR could prove useful to gain insight into concrete radical-related degradation pathways by characterizing short-lived intermediate radical products via spin trapping, this approach is currently rarely used in formulation development. Its labor-intensiveness, low throughput, and need for expert knowledge make EPR spectroscopy a nonstandard analytic method for the pharmaceutical industry. To solve troubleshooting issues as presented in this study, EPR is worth to be considered and used. Two studies regarding the application of EPR to polysorbate solutions are available. Lam et al. (2011) used EPR to detect radicals, focusing on their effect on protein oxidation rather than polysorbate degradation (Lam et al., 2011). The authors of the second study, Doyle et al. (2019), declared their results as "inconclusive" (Doyle et al., 2019). Polysorbate degradation products were observed in the course of this study by complementary methods, but strangely no radicals were detected using EPR or nuclear magnetic resonance spectroscopy (Doyle et al., 2019).

We applied EPR spectroscopy in combination with spin trapping (Timmins et al., 1999; Bauer et al., 2018) for the detection of short-lived free radicals with a half-life on the order of nanoseconds. Many radicals are too transient to be detected directly with EPR. Therefore, molecules that catch and accumulate these radicals (spin traps) need to be introduced. In contrast to spin probes and spin labels, spin traps are no radicals themselves and therefore "EPR silent". Spin traps react (k_T) with free radicals and form more stable and long-lived (half-lives up to several minutes or even hours (Marriott et al., 1980a; Stolze et al., 2000)) spin adducts that can be detected using EPR (see Fig. 1). By selection of a suited spin trap, distinguishing oxygen-, carbon-, nitrogen- and sulfur-centered radials is possible (Haywood, 2013). For this feasibility study, we chose 5,5-dimethyl-1-pyrroline-N-oxide (DMPO) which is perhaps the most frequently used nitrone spin trap (Suzen et al., 2017). It has the advantage of good solubility in aqueous solutions and reacts to a stable, sterically hindered nitroxide radical upon radical trapping (Fig. 1). For trapped $HO^{\bullet}$ the half-life of the formed radical adduct is 54 s in PBS (phosphate-buffered saline) at pH 7.0 (Villamena and Zweier, 2002). Especially oxygen-centered radicals such as $O_2^{\bullet-}$ and $HO^{\bullet}$ are trapped well with DMPO and can be detected in the spectra recorded by EPR (Fig. 1) (Villamena, 2017; Clément and Tordo, 2007). In an aqueous solution, highly reactive $HO^{\bullet}$ radicals play a more prominent role as described below. The half-life of $HO^{\bullet}$ radicals is on the order of nanoseconds and cannot be measured directly with EPR without an additional marker such as a spin trap (Phaniendra et al., 2015).

2. Prerequisites for meaningful radical detection

The trained experimenter must be aware that the detected signal does not only depend on the radicals that are present in the solution, but also on the radical-marker-interaction. This phenomenon will affect all marker-based assays like e.g. the Fox assay or EPR analysis. Therefore, it is essential to understand the mechanisms of spin trapping for a critical and realistic interpretation of the results obtained by EPR.

Reliable quantification of radical species requires the following conditions:

1. Co-location of the radical and the spin trap.
2. Quantitative formation of the spin adducts.
3. Unique and specific spectral pattern of the spin adduct to a specific radical.
4. High stability of the formed spin adducts, e.g. no decay during the time of the experiment.

Although many studies on quantitative EPR spin trapping have been published, these requirements are often not met. The first condition that the spin trap needs to be at the same place as the radical seems trivial, but might not always be the case. This can be found in samples of highly viscous solutions such as bulk PS or highly concentrated pharmaceutical formulations (Blaffert et al., 2018) or the location in different microenvironments (e.g. lipophilic or hydrophilic domains or phases). In many pharmaceutical formulations, viscosities of around 10 mPa·s are common, but higher values up to 150 mPa·s and above were also reported (Rodrigues et al., 2021). Bulk PS80 possesses a viscosity of up to 400 cSt according to the CoAs (certificates of analysis) (Table S1). This value corresponds to a dynamic viscosity of about 420 mPa·s assuming a density of 1.06 gcm^{-3} for PS80 and is orders of magnitude higher than the one for aqueous solutions (viscosity of water approx. 1 mPa·s (Kestin et al., 1978)). If the experimental EPR protocol is not carefully designed, this might lead to different outcomes in bulk and diluted PS80 not solely due to the difference of "chemical" partners available (water), but also because of the "physical" difference of these solutions.

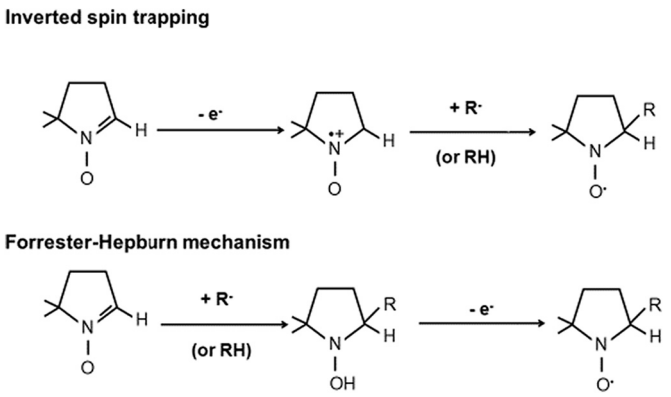

Scheme 2. Generation of DMPO-radical adducts via alternative reaction pathways such as inverted spin trapping and Forrester-Hepburn mechanism.

The second requirement is the quantitative formation of the spin adduct. This depends, in addition to the required co-location of both molecules, on their reactivity. The most reactive radical is the hydroxyl radical $HO^{\bullet}$ which reacts at a diffusion-controlled rate ($k > 10^9\ M^{-1}{\cdot}s^{-1}$) (Finkelstein et al., 1980; Hawkins and Davies, 2014; Goldstein et al., 2004). However, for superoxide radicals $O_2^{\bullet-}$ or their protonated form $HOO^{\bullet}$ the reactivity is 6 to 9 orders of magnitude lower (Buettner and Mason, 1990; Haywood, 2013; Finkelstein et al., 1980; Hawkins and Davies, 2014; Goldstein et al., 2004). The huge differences in reactivity imply a very different trapping efficacy and make the detection of superoxide radicals difficult. In addition, the (pH-dependent) protonation status of the radical species (e.g. $O_2^{\bullet-}$/ $HOO^{\bullet}$) impacts the reaction constant k_T of the radical with the spin trap (Finkelstein et al., 1980; Hawkins and Davies, 2014; Allouch et al., 2007). For example, for DMPO, the rate constant k_T for $HO^{\bullet}$ is orders of magnitude higher than the one for $HOO^{\bullet}$ ($2.7{\cdot}10^9$ vs. $4.03{\cdot}10^5\ mol^{-1}{\cdot}dm^3{\cdot}s^{-1}$) (Marriott et al., 1980b; Lauricella et al., 2004). Various authors have proposed the following increasing order of reactivity of nitrones, such as DMPO, with radical species (Villamena, 2017; Clément and Tordo, 2007):

$$NO^{\bullet} < O_2^{\bullet-} < HOO^{\bullet} < HS^{\bullet} < H_3C^{\bullet} < HO^{\bullet}.$$

The low reactivity requires high concentrations of the spin trap, which might interfere with the kinetics of radical reactions, e.g. the dismutation of superoxide (Britigan et al., 1991).

The third requirement, a specific spectrum for the trapped radical is not always met. For example, trapped superoxide might have comparable EPR spectra with other peroxides (Buettner and Mason, 1990). In such cases, further attempts to identify the radicals are necessary, e.g. the addition of superoxide dismutase (Buettner and Mason, 1990) or further analytical tools (e.g. HPLC/MS) (Lardinois et al., 2008; Qin et al., 2020). However, these measures will increase the complexity even

more.

The fourth factor is the reaction specificity and the possibility of other competitive, nonradical reactions. A common bias of radical assays is the reaction with metals that can catalyse alternative reaction pathways (Bagryanskaya et al., 2015). In the context of EPR, alternative pathways are inverted spin trapping or the so-called Forrester-Hepburn mechanism (Scheme 2) (Leinisch et al., 2011).

For inverted spin trapping, the one-electron oxidation is followed by a nucleophilic attack, whereas the reaction takes place in reverse order for the Forrester-Hepburn mechanism. Both mechanisms lead to the same nitroxide radical as for trapping an actual free radical and therefore causing false-positive contributions to the EPR signal. The intermediate product of the Forrester-Hepburn mechanism is a hydroxylamine which is EPR-silent.

Last, but not least, the half-life of the spin adducts or decay rate k_D must be considered. This rate varies between the different adducts and the surrounding environment. The DMPO-trapped $HO^{\bullet}$ is much more stable than a trapped $O_2^{\bullet -}$ (hours vs. seconds) (Haywood, 2013). Other authors reported low stability values for both hydroxyl and superoxide spin adducts (half-life only a few minutes) (Bartosz, 2006). The instability leads towards a certain bias of the proportion of stable spin adducts since they will accumulate compared to short-lived adducts. The spin adduct stability could also be affected by other radicals and substances contained in the sample, e.g. antioxidants (e.g. ascorbic acid) can reduce the radical adducts to diamagnetic species.

Additional factors affecting radical detection using EPR and spin trapping are:

- the optimization of the settings of the EPR set-up to circumvent problems with the signal-to-noise ratio.
- contaminations of the spin trap with degradation compounds that will bias the results
- temperature-induced effects during incubation

The latter is very critical as the temperature can influence the number of detected radicals by either enhancing radical initiation and propagation reactions k_{Dis} or the spin trapping rate k_T. It is not possible to unambiguously measure those two effects on their own. Due to these reasons, the diligent evaluation of the trapping kinetics is key before starting systematic studies of radical detection in specific samples.

In this feasibility study, we evaluated if and to which extent EPR spectroscopy in combination with the spin trap DMPO can be applied to detect and identify free radicals present in bulk and aqueous solutions of PS80 and their role in polysorbate degradation as proposed in the literature (EPR Application Spotlight: Analyzing the Shelf Life of Polysorbates for the Pharmaceutical Industry, 2019). Based on that knowledge the origins of the radicals might be identified and potential mitigation strategies might be developed to ensure a stable formulation. A protocol is proposed that consciously deals with the challenges and pitfalls of spin trapping and its kinetics to generate meaningful results. The variation of the ratio of different radical types between different samples and its evolution with time under different conditions was evaluated. We compared different batches and quality grades of PS80 from different suppliers to learn whether certain quality grades or products of a certain manufacturer and batches provide any advantages regarding the radical burden compared to other products.

3. Materials and methods

3.1. Materials

Different quality grades and batches of polysorbate 80 were purchased from Croda (International Plc. Snaith, UK): (i) high purity (HP), (ii) super-refined (SR), and (iii) all-oleate (AO) as well as from Nanjing Well (Nanjing, China): (iv) china grade (CG) (see Table S1). DMPO (5,5-Dimethyl-1-Pyrroline-N-Oxide) was purchased from Dojindo Molecular Technologies (Rockville, US), Tempol (4-Hydroxy-2,2,6,6-tetramethylpiperidine-1-oxyl) in a solid crystalline form from Sigma-Aldrich Chemie GmbH (Taufkirchen, Germany). Glass capillaries (Blaubrand) and Critoseal for the EPR experiments were obtained from Brand GmbH & Co. KG (Wertheim, Germany).

3.2. Sample preparation

PS80 bulk material (5 g) was weighed directly into a volumetric flask with a volume of 50 ml and filled with double distilled water to prepare 10% (*w/v*) solutions (pH 6). The solution was placed on a magnetic stirrer at room temperature until PS80 was completely dissolved. The stirring bar was removed. Aliquots of the solution were transferred to ready-to-use glass vials (type I glass), overlayed with nitrogen to decrease exposure to oxygen, and closed with a rubber stopper and an aluminum crimp cap. The aliquots were stored frozen at −20 °C until use.

PS80 bulk material was aliquoted and stored with a nitrogen overlay at 2–8 °C until use as recommended by Croda on their CoAs. This procedure was used for all tested PS80 quality grades.

The PS80 samples and spin traps were equilibrated to room temperature (RT ≈ 25 °C) before measurement. 300 µl of the sample were mixed with 3 µl of DMPO and vortexed for 1 min. Then the samples were transferred to 100 µl capillaries in the case of bulk PS and 50 µl capillaries in the case of 10% (*w/v*) PS80 solutions. The capillaries were sealed with Critoseal.

3.3. Temperature stability study

Samples of 10% (*w/v*) solution of different PS80 batches were stored at 40 °C for selected times (0, 1, 4, 6, 24, 48, and 72 h). DMPO was added to the aliquots in the glass vials, incubated together with the samples at 40 °C, and measured directly after drawing the DMPO containing samples from the drying cabinet. After incubation, the samples were transferred to 50 µl capillaries in the case of 10% (*w/v*) PS80 solutions. The capillaries were sealed with Critoseal and the measurement started.

3.4. Electron paramagnetic resonance (EPR)

All EPR experiments were performed with a MiniScope MS 200 spectrometer from Magnettech GmbH (Germany) using the software MiniScope 1.0.0.1133. The gain mantisse was set to 7, the gain exponent to 2, the B_0-field to 336.5454 mT, and the sweep to 7 mT. For the adjustable parameters, the following optimized settings for an improved signal-to-noise ratio were used: modulation was set to 0.120 mT, the sweep time to 180 s, and the microwave attenuation power to 8 dB.

Selected measurements with the spin probe Tempol were performed with a Bruker MS-5000, Software ESRStudio 1.74.0 B_0-field to 337.5 mT, and the sweep to 10 mT, modulation 0.02 mT, sweep time 60 s, microwave power 5 mW and the MS 200 B_0-field to 336.5 mT, and the sweep to 10 mT, modulation 0.02 mT, sweep time 60 s for comparison of signal-to-noise ratio.

The measurements were performed at room temperature (RT ≈ 25 °C). The capillary was positioned in the resonator of the instrument, the spectrometer was tuned followed by starting the measurement. Three single spectra were recorded for each sample and sampling time point. The capillaries containing the samples were stored at ambient temperature (protected from light) between measurements at different time points.

3.5. EPR data analysis

The recorded spectra were baseline corrected, fitted, and double integrated with the program EasySpin for Matlab (Mathworks). The EasySpin function “Garlic” was used for simulation in the fitting procedure (Stoll and Schweiger, 2006). The weight and partially the

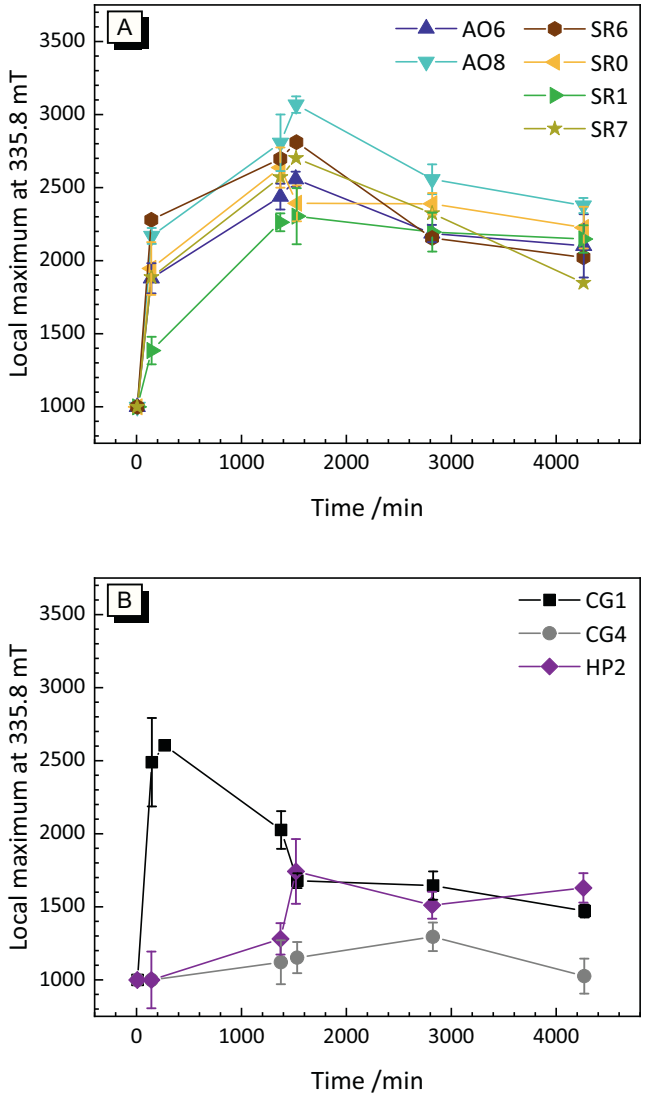

Fig. 2. Spin trapping kinetics of DMPO in PS80 bulk material. The signal intensity at 335.8 mT at different time points is recorded for different qualities of bulk PS80 and batches thereof: CG, AO, SR, and HP. Data represent averages of three subsequent single measurements of the same sample and their corresponding standard deviations.
HP: High Purity, CG: China grade, AO: All-Oleate, SR: Super-Refined.

hyperfine splitting were varied, whereas the linewidth was fixed. There is only a limited number of variables in the EasySpin fitting routine. All samples were fitted with the same starting values. To determine the ratios, the values are normalized to 100% as advised by the software manual. The presented values and error bars are the mean and the standard deviation from the fitting results of three measurements. The total uncertainty is larger due to the noise and the different trapping efficiency of the spin trap.

The data evaluation of local maxima and the figures were made using OriginPro2019 (OriginLab). The data points are averages of three measurements.

4. Results and discussion

4.1. Spin trapping in polysorbate samples

The capability to detect radicals with EPR strongly depends on the interaction of the spin trap with the sample as outlined in the introduction. Spin traps with linear chemical structures were not tested, since cyclic ones are recommended due to their better trapping properties and adduct stability (Clément and Tordo, 2007). To obtain meaningful results, we evaluated the effect of incubation time on the signal quality to perform our measurements at maximal signal intensity.

We started with the evaluation of bulk material of PS80 of different quality grades and batches. Calculation of the absolute concentration of detected radials by double integration was not possible for these samples, since the signal-to-noise ratio was too low and results were inaccurate (see Fig. S1, supporting information, SI). Differences in the amplitude mirror differences in the quantity of detected radicals between the samples. For this reason, we started with a more qualitative comparison between the samples to investigate for general trends of the spin trapping kinetics.

A pronounced and well-defined local maximum at 335.8 mT was reliably determined in all preliminary experiments during the optimization process and therefore chosen as representative for the examined spectra (data not shown). Using averaged baseline subtraction, it was

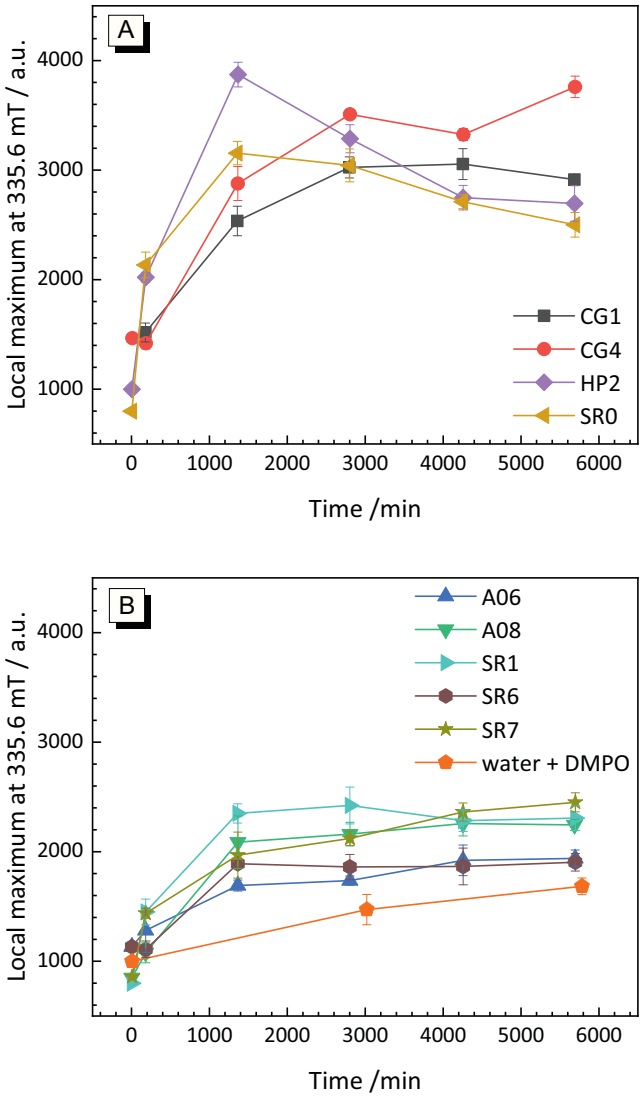

Fig. 3. Spin trapping kinetics of DMPO in aqueous solutions containing 10% (*w/v*) PS80. The signal intensity at 335.6 mT at different time points is recorded for various qualities of PS80 and batches thereof. The trapping kinetics are either fast (A) or slow (B) for CG, AO, SR, and HP grade PS80. For reference, we added DMPO in pure water. Data represent averages of three measurements.
HP: High Purity, CG: China grade, AO: All-Oleate, SR: Super-Refined.

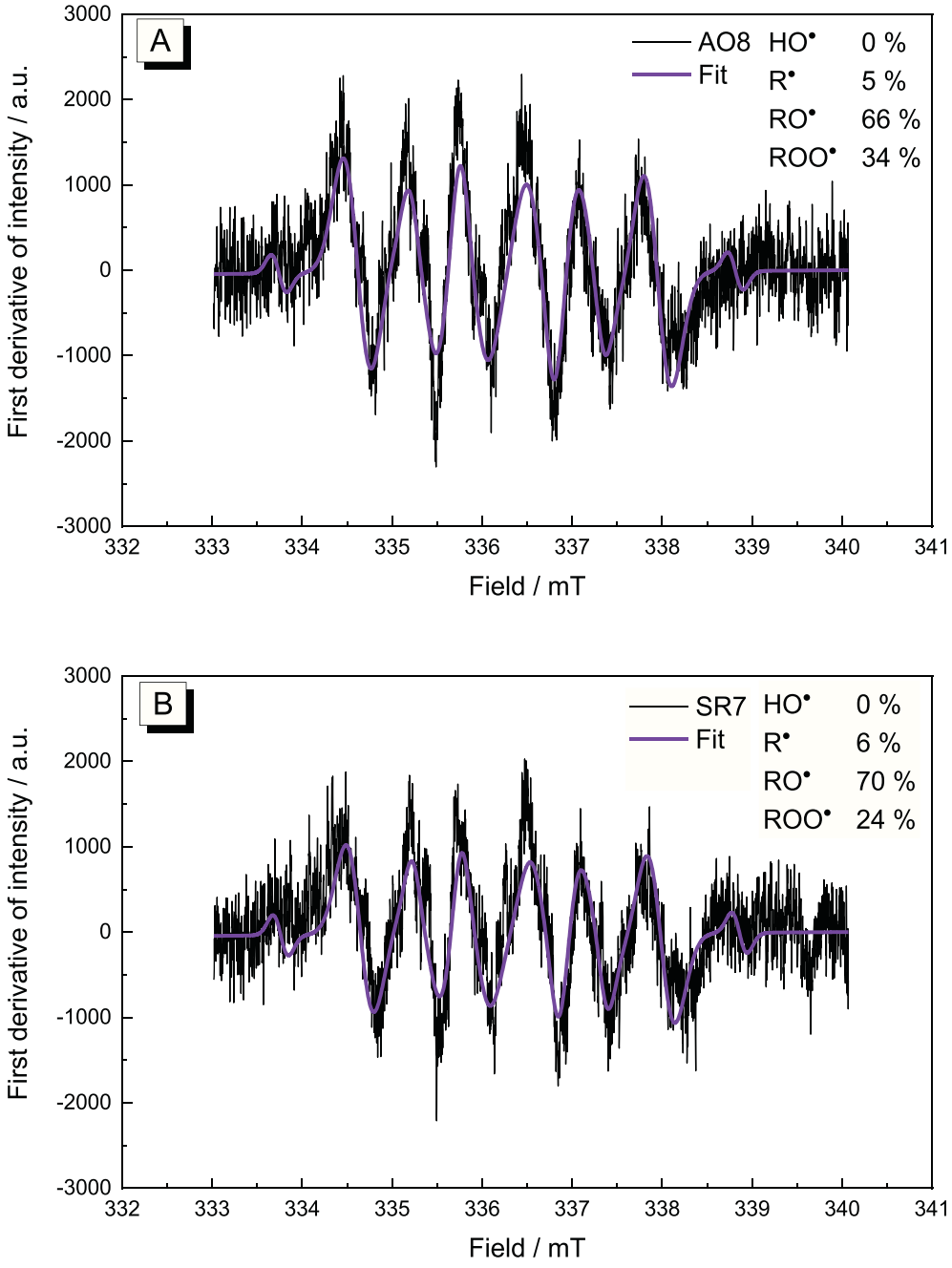

Fig. 4. Exemplary fitting of two samples of bulk material of PS80: AO8 (A) and SR7 (B). The percentages of the different radical species contributing to the signal are determined (see insert).
AO: All-Oleate, SR: Super-Refined.

possible to set the baseline near zero and to provide an equal determination of local maxima. As shown in Fig. 1 (dashed line), the signal at this field intensity mainly results from $R^{\bullet}$ and $ROO^{\bullet}$, while the signal contributions of $RO^{\bullet}$ and $HO^{\bullet}$ are negligible/close to the baseline.

To evaluate the day-to-day variability of the set-up, we performed measurements with Tempol (Fig. S2, SI). Tempol is a very stable probe. For Tempol and other nitroxides, the limit of detection was around 0.5 μM for a single scan (and even lower by multiple scanning). The signal intensity of the same sample was measured at 335.8 mT in triplicates. The standard deviations for three subsequent measurements on the same day range from 1.6 to 3.0% of the average value of these three measurements. The maximum deviation between the minimum and the maximum value ranged from 3.8 to 8.9% of the average value. This gives us an orientation regarding the aqueous PS samples. Stronger variations are expected for the DMPO-PS system.

The spin trapping kinetics for different quality grades of the bulk material were recorded (Fig. 2). There was no absolute unique trend of the intensity signal observable over time, but most samples showed an intensity maximum at approx. 1500 min independent of the PS80 quality grade. The standard deviations per sampling time point varied between 2 and 13% of the corresponding average value. The existence of a temporal maximum of signal intensity suggests, that initially, the trapping rate k_T is higher than the decay rate k_D of the spin adducts, but the opposite is true for later time points.

In general, no extreme differences are observed for the various batches and grades of the bulk material with exception of three samples:

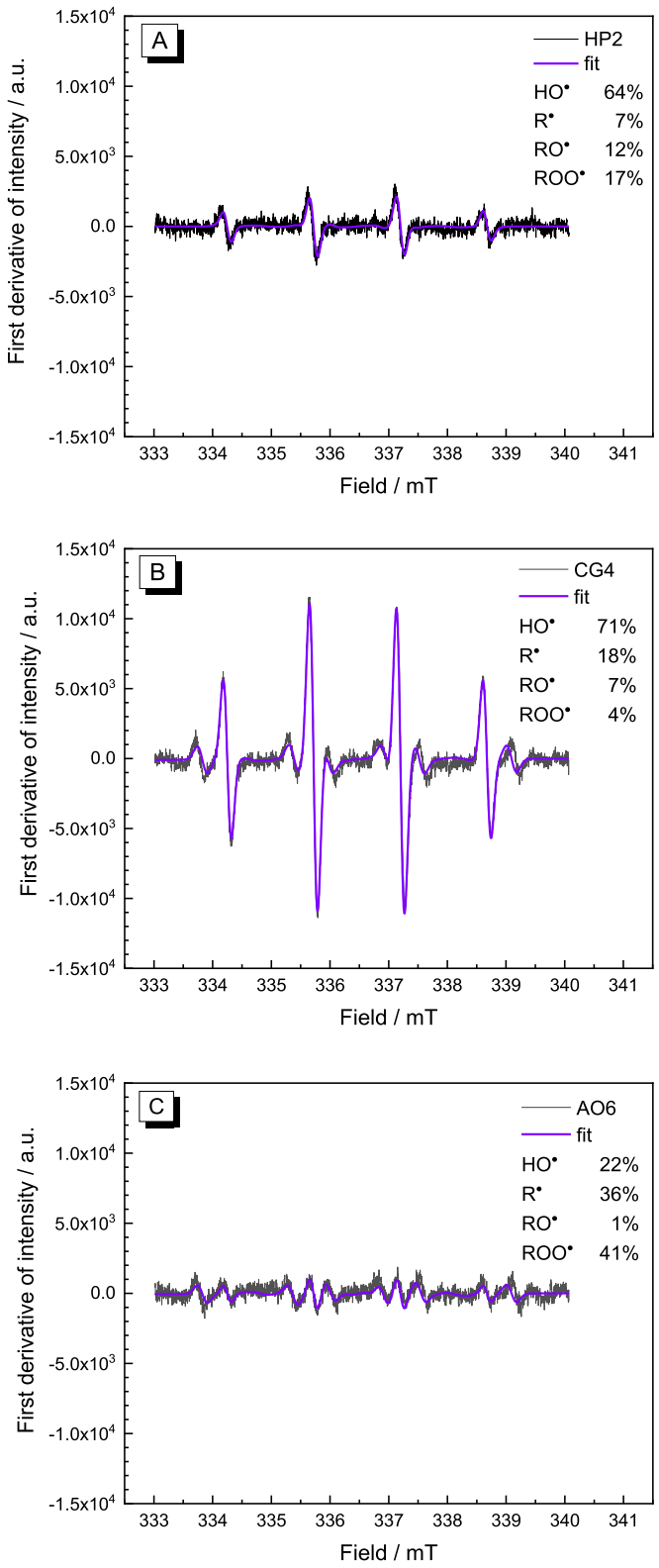

Fig. 5. Exemplary fitting of 10% (*w/v*) PS80 samples. (A) HP2 (RT / 2 d), (B) CG4 (RT / 5 min), and (C) AO6 (sample stored at 40 °C / 1 h). The percentages of the different radical species contributing to the signal are determined (see insert). The variance of the intensity of the spectra shows a certain randomness of the presence of radicals.
HP: High Purity, CG: China grade, AO: All-Oleate.

CG4, HP2, and CG1. All three samples show lower signals after about 1500 min of incubation compared to the other samples. Their signal still ranges around 1500 a.u., compared to intensities above 2500 a.u. for the other samples (Fig. 2, right). This result seems counter-intuitive at first. Considering that unsaturated FAs are prone to radical attack and CG contains the highest amount of these FAs, while HP2 contains the lowest amount of them. Related to the manufacturing date, HP2 and CG1 are the earliest batches (i.e. the batch with the highest shelf-life), so a low radical content in relation to the total age would be an explanation. On the other hand, AO6 is the third youngest batch, showing a much higher signal than CG4 after 1500 min (2557 a.u. vs. 1153 a.u.). There was no correlation between the maximal signal intensity observed and any other parameters listed in the CoA such as the peroxide value or the oleic acid content. For example, AO6 possesses the highest peroxide value (0.7 (mEq O_2)·kg^{-1}), but its signal kinetics do not differ much from the ones of the SR samples with a peroxide value of 0.2–0.5 (mEq O_2)·kg^{-1}. All of this indicates that there might be more factors to consider than just the quality grade and the information provided by the CoAs. This observation is also confirmed by the rest of the presented data.

The kinetics of the 10% (*w/v*) PS80 solutions showed an interesting trend (Fig. 3) by monitoring the signal at 335.6 mT corresponding mainly to HO•. The kinetic profile can be divided into two "regions". A set of PS80 samples shows a fast increase in the signal of that later plateaus (Fig. 3A), while the other set of the samples showed a slow increase (Fig. 3B). There is currently no obvious reason for this phenomenon. The standard deviations ranged from 2 to 15%, while the majority of the values were between 2 and 5%. Therefore, this range is slightly higher than the upper limit of the Tempol test measurement but still close enough to assume good comparability between measurements performed on different days. No direct correlation regarding the signal intensity between the bulk PS80 material and the 10% (*w/v*) PS80 solutions is found for the different quality grades and batches (Fig. 3), e.g. HP2 gives a low signal in bulk material but a very high signal in the 10% (*w/v*) PS80 solution. For both AO batches we observe the reverse trend.

Regarding the reasoning of a diffusion-limited reaction of the spin trap with the radical, this is not completely surprising. In general, a steeper increase of the intensity-time curve is seen for samples represented in Fig. 3A compared to the samples shown in Fig. 3B. This can have two reasons. Firstly, if comparatively the concentration of radicals present in the solution is higher, then this can lead to an increase in the total signal intensity. The steeper increase can be explained by the following. In the case, the radical concentration present in the solution is higher, this increases theoretically the probability that a spin trap reacts faster with a radical to an EPR-detectable adduct. A second aspect related to the steep increase is linked to the spin-trapping kinetics. Assuming that the actual radical content is comparable to the one in the bulk material, the trapping kinetics is speeding up by the reduction of the viscosity in an aqueous solution. As outlined in the introduction, spin-trapping is diffusion-limited, therefore a faster diffusion and reaction rate will lead to a faster accumulation of stable, EPR-measurable spin adducts. In reality, both effects might be present and interfere with each other.

4.2. Possible radical composition of polysorbate samples

To learn more about the radical species that are present in the different solutions, we applied the EasySpin function "Garlic" for simulation and fitting our data (Stoll and Schweiger, 2006). Exemplary data for bulk material and 10% (*w/v*) PS80 solutions at room temperature are shown in Fig. 4 and Fig. 5.

The spectra of the diluted samples (10% (*w/v*)) were more defined than the ones of the bulk material. The peaks of the aqueous diluted solutions can be associated easily with dominating HO-DMPO trapping adducts (see Fig. 1). A certain preference of DMPO for this type of radical is undeniable and agrees with literature (Villamena, 2017; Clément and Tordo, 2007). The spectra detected in 10% (w/v) solutions of PS80 differ

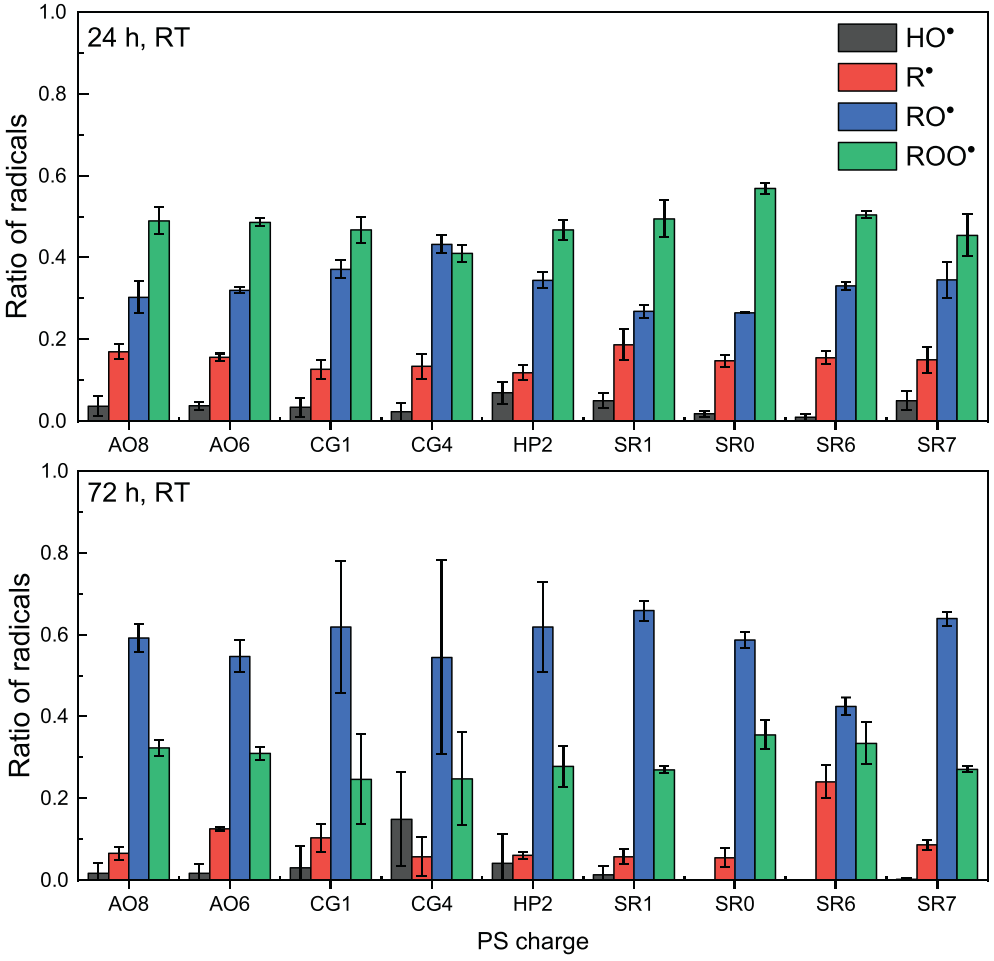

Fig. 6. Normalized relative ratios of PS80 bulk material with DMPO after storage for 24 h and 72 h at room temperature (RT ≈ 25 °C). The main species present shifts from ROO• to RO• within that time frame.
HP: high purity, CG: China grade, AO: All-Oleate, SR: Super-Refined.

strongly in their intensity, indicating that the bulk material that is used to prepare them, might be at different stages of the radical propagation (see Scheme 1).

Although the signal intensity differs slightly for the two bulk samples in Fig. 4, the fitting results in ratios for the different radical species that are of a comparable order of magnitude, with RO• showing the highest ratio with approx. 70%. This also holds for all other samples (Fig. 6). The ratios of the radicals are independent of the tested PS80 quality grade or batch. After 24 h, ROO• (approx. 50–60%) and RO• (30–45%) radicals are the dominating species in bulk PS80 (Fig. 6). After 72 h, the distribution of fractions reverses: 20–30% ROO• and 50–60% RO•. R• and HO• radicals play a subordinate role (Fig. 6). The low amount of HO• might be linked to the low water content in bulk material (<0.1% water). The differences in composition regarding the FAs or the other parameters listed in the CoA do not seem to be pronounced enough to cause substantial differences in the radical ratios.

For diluted samples, a different pattern is observed (Fig. 7). Again, the radical ratios are comparable for the different tested batches and quality grades of PS80, indicating a certain independence of these parameters. With 70–80%, HO• is the dominating species after 24 h in solution and after 48 h as well. The patterns of the bulk material (Fig. 6) and the diluted samples (Fig. 7) differ strongly, underlining the importance of water as a reaction partner during radical propagation. Still, the question remains, which radicals that are present in the bulk material form the radicals detected in the aqueous solutions. The high amounts of HO• could also originate from HOO• since DMPO-OOH adducts are less stable and can decompose to DMPO-OH adducts (Villamena, 2017). To clarify this, mass spectrometry-based analysis of spin adducts would be necessary, however, this is out of the scope of this study.

4.3. *Temperature stability study*

The stability of biopharmaceutical products is evaluated by long-time storage at 40 °C. Therefore, we checked the radical content in aqueous solutions at elevated temperatures as well. Firstly, we incubated the samples at elevated temperatures and added the DMPO right before the measurement. Unfortunately, by following this protocol we did not obtain a sufficiently well-defined signal that we could further analyze (data not shown). Therefore, we decided to add DMPO during sample preparation to the samples and incubate the spin trap together with the PS (Fig. 8). This procedure has a certain bias. The spin trapping kinetics and the stability of the spin adducts might be affected by the increased incubation temperature as well. We are not aware of any reference measurements that would allow us to disentangle these effects. Therefore, the following results need to be considered rather as estimates than absolute values. The increase in signal intensity with incubation time is clear (Fig. 8A). Interestingly, we do not observe a tremendous change in the ratio of the radical species after 4 h for the tested qualities although the total amount seems to increase when having a look at the EPR raw data. The ratios of the radicals follow a similar trend as for the aqueous solutions stored at 25 °C (Fig. 7): 50–80% HO• and contributions of up to 20% from ROO• and RO•. The

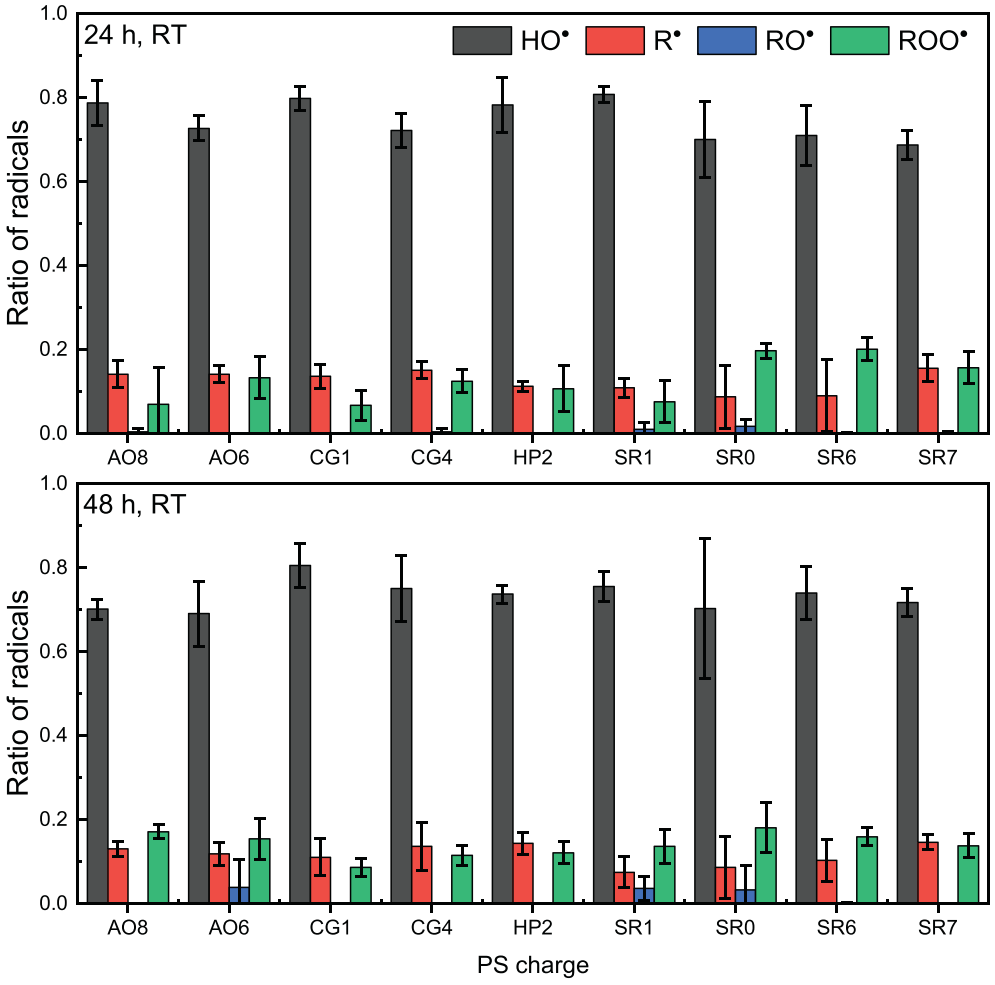

Fig. 7. Normalized relative ratios of PS80 in 10% (*w/v*) solutions with DMPO after storage for 24 h and 48 h at room temperature (RT ≈ 25 °C). The main species is HO• which stays constant.
HP: High Purity, CG: China grade, AO: All-Oleate, SR: Super-Refined.

measurement at 24 h corresponds to the determined intensity maxima at around 1500 min. And indeed, after that time the signal does not change much anymore. No difference that goes beyond normal sample-to-sample variations was observed between the samples with ambient air and the ones with nitrogen overlay (Fig. 8 B-D). Fig. S3 (SI) shows exemplarily a direct comparison of the radical ratio composition of selected 10% (*w/v*) aqueous PS80 dilutions at 25 °C and 40 °C. No relevant difference in the radical ratio distribution is noted for storing the PS80 samples 24 h at both temperatures (Fig. S3, SI).

5. Conclusions

Free radicals are formed in a variety of stress conditions or manufacturing processes and can strongly affect the drug product quality. With EPR (Electron Paramagnetic Resonance) spectroscopy, it was possible to detect transient radicals in PS80 solutions. Radicals such as HO•, R•, RO• and ROO• could be identified in bulk PS80 material as well as in aqueous PS80 dilutions (10% *w/v*) using the spin trap DMPO.

EPR has the advantage that it allows to detect radicals even at low concentrations, although a direct quantification was not suitable with our data due to pronounced uncertainties in the double integral. The signal-to-noise ratio of unfiltered EPR spectra is often too low and fluctuations of the baseline and obtained signals are too high to achieve acceptable results with double integration. Therefore, calculation of detected radical concentration was not performed and only relative comparisons (ratios) of the detected radical amount between the samples concerning the signal amplitude or local maxima were practicable.

Regarding the identification of the radical species and their ratios, differences were observed for the raw material compared to the 10% (*w/v*) PS80 solutions. While for the bulk material mainly ROO• and RO• species could be detected (in total 80–90%), in the 10% (*w/v*) solutions of PS80 mainly HO• radicals were detected (70–80%). Comparing different PS80 quality grades and different batches, the ratio of the radicals was similar for all tested PS80 samples in bulk material or aqueous solutions independent of the PS80 quality grade. No general pattern that connects the PS quality grade or other parameters listed in the CoA with the radical content was obvious.

Regarding the interpretation of the results, one should always keep in mind that the trapping reaction of the spin trap leading to radical adduct formation and adduct decay is monitored and not the radical formation and radical decay itself. Direct conclusions on the radical content should be drawn with care. Radical formation in PS80 containing solutions as well as the trapping kinetics are both strongly time and temperature-dependent, not clearly defined, and therefore difficult to predict.

The proposed EPR feasibility study shows that EPR provides complementary information, currently not been obtained by other methods, and thus supports the elucidation of the role of radicals in the degradation of polysorbates. EPR allows estimating the ratio of the present radical species in polysorbate 80, information that is not easily obtained

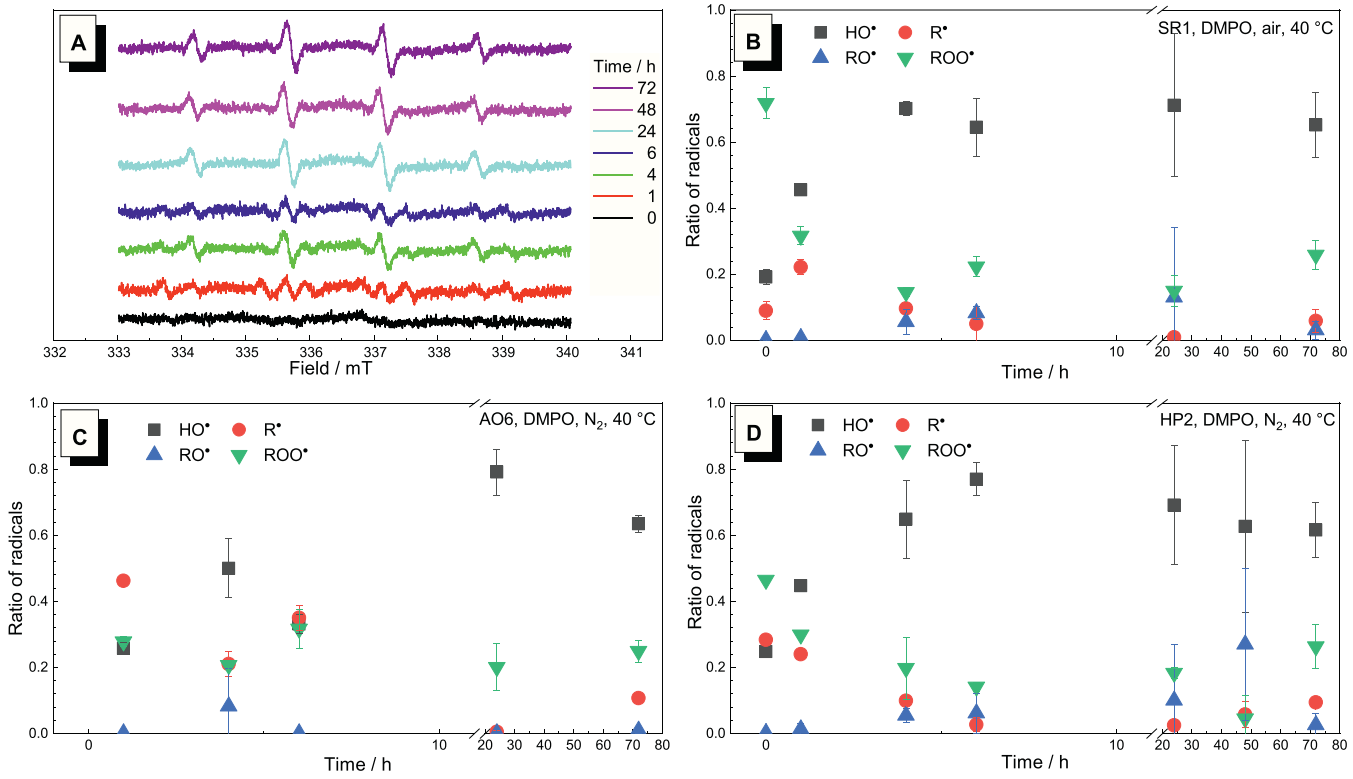

Fig. 8. Radical content at elevated temperature (40 °C) over time in 10% (*w/v*) solutions A) EPR raw data for AO6, 10% (*w/v*) PS80 solution B) Normalized fractions of the different radicals in SR1 with ambient air overlay C), D) Normalized fraction of the different radicals in AO6 and HP2 with nitrogen overlay. The spin trap DMPO was incubated together with the PS solutions at 40 °C for the shown amount of time.
HP: High Purity, CG: China grade, AO: All-Oleate, SR: Super-Refined.

by e.g. using biochemical assays. All in all, the identification and reliable quantification of free radicals remains a tedious scientific task. Further efforts are required to adopt this approach to the needs of the pharmaceutical industry.

Author contributions

All authors jointly designed the study, discussed the results commented, and reviewed the manuscript.

M.-L.T. and H.K. Data curation, formal analysis, visualization

J.J.M. wrote the first draft of the manuscript.

J.B. and P.G. were responsible for the concept, budget, project administration, and supervising.

K.M. supervised the work and finalized the manuscript.

Declaration of Competing Interest

The authors declare that they have no known competing financial interests or personal relationships that could have appeared to influence the work reported in this paper.

Acknowledgment

We gratefully acknowledge, Oliver Burkert, Felix Halbach, Josef Hartl, Stefan Carle for discussions and Holger Thie and Kerstin Walke for support, as well as Tim Diederichs for proofreading. We thank Dariush Hinderberger for the possibility to conduct comparison EPR measurements in his laboratory.

Appendix A. Supplementary data

Table with an overview of CoAs of PS80 charges, Tempol references.

Supplementary data to this article can be found online at [https://doi.org/10.1016/j.ijpx.2022.100123].

References

Allouch, A., Lauricella, R.P., Tuccio, B.N., 2007. Effect of PH on superoxide/hydroperoxyl radical trapping by nitrones: an EPR/kinetic study. Mol. Phys. 105 (15–16), 2017–2024. https://doi.org/10.1080/00268970701494024.

Bagryanskaya, E.G., Krumkacheva, O.A., Fedin, M.V., Marque, S.R.A., 2015. Chapter fourteen development and application of spin traps, spin probes, and spin labels. Methods Enzymol. 563, 365–396. https://doi.org/10.1016/bs.mie.2015.06.004.

Bartosz, G., 2006. Use of spectroscopic probes for detection of reactive oxygen species. Clin. Chim. Acta 368 (1–2), 53–76. https://doi.org/10.1016/j.cca.2005.12.039.

Bates, T.R., Nightingale, C.H., Dixon, E., 1973. Kinetics of hydrolysis of polyoxyethylene (20) sorbitan fatty acid ester surfactants. J. Pharm. Pharmacol. 25 (6), 470–477. https://doi.org/10.1111/j.2042-7158.1973.tb09135.x.

Bauer, N.A., Hoque, E., Wolf, M., Kleigrewe, K., Hofmann, T., 2018. Detection of the formyl radical by EPR spin-trapping and mass spectrometry. Free Rad. Bio. Med. 116, 129–133. https://doi.org/10.1016/j.freeradbiomed.2018.01.002.

Bergh, M., Shao, L.P., Hagelthorn, G., Gäfvert, E., Nilsson, J.L.G., Karlberg, A., 1998. Contact allergens from surfactants. atmospheric oxidation of polyoxyethylene alcohols, formation of ethoxylated aldehydes, and their allergenic activity. J. Pharm. Sci. 87 (3), 276–282. https://doi.org/10.1021/js9704036.

Blaffert, J., Haeri, H.H., Blech, M., Hinderberger, D., Garidel, P., 2018. Spectroscopic methods for assessing the molecular origins of macroscopic solution properties of highly concentrated liquid protein solutions. Anal. Biochem. 561, 70–88. https://doi.org/10.1016/j.ab.2018.09.013.

Borisov, O.V., Ji, J.A., Wang, Y.J., 2015. Oxidative degradation of polysorbate surfactants studied by liquid chromatography–mass spectrometry. J. Pharm. Sci. 104 (3), 1005–1018. https://doi.org/10.1002/jps.24314.

Britigan, B.E., Roeder, T.L., Buettner, G.R., 1991. Spin traps inhibit formation of hydrogen peroxide via the dismutation of superoxide: implications for spin trapping the hydroxyl free radical. Biochim. Biophys. Acta Bba - Gen Subj. 1075 (3), 213–222. https://doi.org/10.1016/0304-4165(91)90269-m.

Buettner, G.R., Mason, R.P., 1990. Oxygen radicals in biological systems part b: oxygen radicals and antioxidants. Methods Enzymol. 186, 127–133. https://doi.org/10.1016/0076-6879(90)86101-z.

Clément, J.-L., Tordo, P., 2007. Electron paramagnetic resonance : volume 20. Electron Paramagnet. Reson. 20, 29–49. https://doi.org/10.1039/9781847557568-00029.

Dahotre, S., Tomlinson, A., Lin, B., Yadav, S., 2018. Novel markers to track oxidative polysorbate degradation in pharmaceutical formulations. J. Pharm. Biomed. 157, 201–207. https://doi.org/10.1016/j.jpba.2018.05.031.

Deiana, L., Carru, C., Pes, G., Tadolini, B., 2009. Spectrophotometric measurement of hydroperoxides at increased sensitivity by oxidation of Fe2+ in the presence of xylenol orange. Free Radic. Res. 31 (3), 237–244. https://doi.org/10.1080/10715769900300801.

Dixit, N., Salamat-Miller, N., Salinas, P.A., Taylor, K.D., Basu, S.K., 2016. Residual host cell protein promotes polysorbate 20 degradation in a sulfatase drug product leading to free fatty acid particles. J. Pharm. Sci. 105 (5), 1657–1666. https://doi.org/10.1016/j.xphs.2016.02.029.

Donbrow, M., Azaz, E., Pillersdorf, A., 1978. Autoxidation of polysorbates. J. Pharm. Sci. 67 (12), 1676–1681. https://doi.org/10.1002/jps.2600671211.

Doyle, L.M., Sharma, A.N., Gopalrathnam, G., Huang, L., Bradley, S., 2019. A mechanistic understanding of polysorbate 80 oxidation in histidine and citrate buffer systems-part 2. PDA J. Pharm. Sci. Technol. https://doi.org/10.5731/pdajpst.2018.009639 pdajpst.2018.009639.

Dwivedi, M., Blech, M., Presser, I., Garidel, P., 2018. Polysorbate degradation in biotherapeutic formulations: identification and discussion of current root causes. Int. J. Pharmaceut. 552 (1–2), 422–436. https://doi.org/10.1016/j.ijpharm.2018.10.008.

Dwivedi, M., Buske, J., Haemmerling, F., Blech, M., Garidel, P., 2020. Acidic and alkaline hydrolysis of polysorbates under aqueous conditions: towards understanding polysorbate degradation in biopharmaceutical formulations. Eur. J. Pharm. Sci. 144, 105211 https://doi.org/10.1016/j.ejps.2019.105211.

EPR Application Spotlight: Analyzing the Shelf Life of Polysorbates for the Pharmaceutical Industry, 2019. White Paper by Bruker.

Etienne, E., Breton, N.L., Martinho, M., Mileo, E., Belle, V., 2017. SimLabel: a graphical user interface to simulate continuous wave EPR spectra from site-directed spin labeling experiments. Magn. Reson. Chem. 55 (8), 714–719. https://doi.org/10.1002/mrc.4578.

Evers, D.-H., Schultz-Fademrecht, T., Garidel, P., Buske, J., 2020. Development and validation of a selective marker-based quantification of polysorbate 20 in biopharmaceutical formulations using UPLC QDa detection. J. Chromatogr. B 1157, 122287. https://doi.org/10.1016/j.jchromb.2020.122287.

Evers, D.-H., Carle, S., Lakatos, D., Hämmerling, F., Garidel, P., Buske, J., 2021. Hydrolytic polysorbate 20 degradation – sensitive detection of free fatty acids in biopharmaceuticals via UPLC-QDa analytics with isolator column. J. Chromatogr. B 1174, 122717. https://doi.org/10.1016/j.jchromb.2021.122717.

Finkelstein, E., Rosen, G.M., Rauckman, E.J., 1980. Spin trapping. kinetics of the reaction of superoxide and hydroxyl radicals with nitrones. J. Am. Chem. Soc. 102 (15), 4994–4999. https://doi.org/10.1021/ja00535a029.

Glücklich, N., Carle, S., Buske, J., Mäder, K., Garidel, P., 2021. Assessing the polysorbate degradation fingerprints and kinetics of lipases – how the activity of polysorbate degrading hydrolases is influenced by the assay and assay conditions. Eur. J. Pharm. Sci. 166, 105980 https://doi.org/10.1016/j.ejps.2021.105980.

Goldstein, S., Rosen, G.M., Russo, A., Samuni, A., 2004. Kinetics of spin trapping superoxide, hydroxyl, and aliphatic radicals by cyclic nitrones. J. Phys. Chem. 108 (32), 6679–6685. https://doi.org/10.1021/jp048441i.

Grabarek, A.D., Bozic, U., Rousel, J., Menzen, T., Kranz, W., Wuchner, K., Jiskoot, W., Hawe, A., 2020. What makes polysorbate functional? Impact of polysorbate 80 grade and quality on IgG stability during mechanical stress. J. Pharm. Sci. 109 (1), 871–880. https://doi.org/10.1016/j.xphs.2019.10.015.

Graf, T., Tomlinson, A., Yuk, I.H., Kufer, R., Spensberger, B., Falkenstein, R., Shen, A., Li, H., Duan, D., Liu, W., Wohlrab, S., Edelmann, F., Leiss, M., 2021. Identification and characterization of polysorbate-degrading enzymes in a monoclonal antibody formulation. J. Pharm. Sci. https://doi.org/10.1016/j.xphs.2021.06.033.

Hawkins, C.L., Davies, M.J., 2014. Detection and characterisation of radicals in biological materials using EPR methodology. Biochim. Biophys. Acta Bba - Gen Subj. 1840 (2), 708–721. https://doi.org/10.1016/j.bbagen.2013.03.034.

Haywood, R., 2013. Encyclopedia of Biophysics, pp. 2447–2453. https://doi.org/10.1007/978-3-642-16712-6_579.

Jaeger, J., Sorensen, K., Wolff, S.P., 1994. Peroxide accumulation in detergents. J. Biochem. Biophys. Methods 29 (1), 77–81. https://doi.org/10.1016/0165-022x(94)90058-2.

Janzen, E.G., 1995. Bioradicals detected by ESR. Spectroscopy 113–142. https://doi.org/10.1007/978-3-0348-9059-5_9.

Jiang, Z.-Y., Hunt, J.V., Wolff, S.P., 1992. Ferrous ion oxidation in the presence of xylenol orange for detection of lipid hydroperoxide in low density lipoprotein. Anal. Biochem. 202 (2), 384–389. https://doi.org/10.1016/0003-2697(92)90122-n.

Kempe, S., Metz, H., Mäder, K., 2010. Application of electron paramagnetic resonance (EPR) spectroscopy and imaging in drug delivery research – chances and challenges. Eur. J. Pharm. Biopharm. 74 (1), 55–66. https://doi.org/10.1016/j.ejpb.2009.08.007.

Kerwin, A.B., 2008. Polysorbates 20 and 80 used in the formulation of protein biotherapeutics: structure and degradation pathways. J. Pharm. Rev. 97 (8), 2924–2935. https://doi.org/10.1002/jps.21190.

Kestin, J., Sokolov, M., Wakeham, W.A., 1978. Viscosity of liquid water in the range −8 °C to 150 °C. J. Phys. Chem. Ref. Data 7 (3), 941–948. https://doi.org/10.1063/1.555581.

Khan, T.A., Mahler, H.-C., Kishore, R.S.K., 2015. Key interactions of surfactants in therapeutic protein formulations: a review. Eur. J. Pharm. Biopharm. 97 (Pt A), 60–67. https://doi.org/10.1016/j.ejpb.2015.09.016.

Kishore, R.S.K., Kiese, S., Fischer, S., Pappenberger, A., Grauschopf, U., Mahler, H.-C., 2011a. The degradation of polysorbates 20 and 80 and its potential impact on the stability of biotherapeutics. Pharm. Res. 28 (5), 1194–1210. https://doi.org/10.1007/s11095-011-0385-x.

Kishore, R.S.K., Pappenberger, A., Dauphin, I.B., Ross, A., Buergi, B., Staempfli, A., Mahler, H., 2011b. Degradation of polysorbates 20 and 80: studies on thermal autoxidation and hydrolysis. J. Pharm. Sci. 100 (2), 721–731. https://doi.org/10.1002/jps.22290.

Knoch, H., Ulbrich, M.H., Mittag, J.J., Buske, J., Garidel, P., Heerklotz, H., 2021. Complex micellization behavior of the polysorbates Tween 20 and Tween 80. Mol. Pharm. https://doi.org/10.1021/acs.molpharmaceut.1c00406.

Kranz, W., Wuchner, K., Corradini, E., Berger, M., Hawe, A., 2019. Factors influencing polysorbate's sensitivity against enzymatic hydrolysis and oxidative degradation. J. Pharm. Sci. 108 (6), 2022–2032. https://doi.org/10.1016/j.xphs.2019.01.006.

Labrenz, S.R., 2014. Ester hydrolysis of polysorbate 80 in MAb drug product: evidence in support of the hypothesized risk after the observation of visible particulate in MAb formulations. J. Pharm. Sci. 103 (8), 2268–2277. https://doi.org/10.1002/jps.24054.

Lam, X.M., Lai, W.G., Chan, E.K., Ling, V., Hsu, C.C., 2011. Site-specific tryptophan oxidation induced by autocatalytic reaction of polysorbate 20 in protein formulation. Pharm. Res. 28 (10), 2543–2555. https://doi.org/10.1007/s11095-011-0482-x.

Lardinois, O.M., Detweiler, C.D., Tomer, K.B., Mason, R.P., Deterding, L.J., 2008. Identifying the site of spin trapping in proteins by a combination of liquid chromatography, ELISA, and off-Line tandem mass spectrometry. Free Rad. Bio. Med. 44 (5), 893–906. https://doi.org/10.1016/j.freeradbiomed.2007.11.015.

Larson, N.R., Wei, Y., Prajapati, I., Chakraborty, A., Peters, B., Kalonia, C., Hudak, S., Choudhary, S., Esfandiary, R., Dhar, P., Schöneich, C., Middaugh, C.R., 2020a. Comparison of polysorbate 80 hydrolysis and oxidation on the aggregation of a monoclonal antibody. J. Pharm. Sci. 109 (1), 633–639. https://doi.org/10.1016/j.xphs.2019.10.069.

Larson, N.R., Wei, Y., Prajapati, I., Chakraborty, A., Peters, B., Kalonia, C., Hudak, S., Choudhary, S., Esfandiary, R., Dhar, P., Schöneich, C., Middaugh, C.R., 2020b. Comparison of polysorbate 80 hydrolysis and oxidation on the aggregation of a monoclonal antibody. J. Pharm. Sci. 109 (1), 633–639. https://doi.org/10.1016/j.xphs.2019.10.069.

Lauricella, R., Allouch, A., Roubaud, V., Bouteiller, J.-C., Tuccio, B., 2004. A new kinetic approach to the evaluation of rate constants for the spin trapping of superoxide/hydroperoxyl radical by nitrones in aqueous media. Org. Biomol. Chem. 2 (9), 1304–1309. https://doi.org/10.1039/b401333f.

Leinisch, F., Ranguelova, K., DeRose, E.F., Jiang, J., Mason, R.P., 2011. Evaluation of the Forrester–Hepburn mechanism as an artifact source in ESR spin-trapping. Chem. Res. Toxicol. 24 (12), 2217–2226. https://doi.org/10.1021/tx2003323.

Marriott, P.R., Perkins, M.J., Griller, D., 1980a. Spin trapping for hydroxyl in water: a kinetic evaluation of two popular traps. Can. J. Chem. 58 (8), 803–807. https://doi.org/10.1139/v80-125.

Marriott, P.R., Perkins, M.J., Griller, D., 1980b. Spin trapping for hydroxyl in water: a kinetic evaluation of two popular traps. Can. J. Chem. 58 (8), 803–807. https://doi.org/10.1139/v80-125.

Moghaddam, A.E., Gartlan, K.H., Kong, L., Sattentau, Q.J., 2011. Reactive carbonyls are a major Th2-inducing damage-associated molecular pattern generated by oxidative stress. J. Immunol. 187 (4), 1626–1633. https://doi.org/10.4049/jimmunol.1003906.

Nayem, J., Zhang, Z., Tomlinson, A., Zarraga, I.E., Wagner, N.J., Liu, Y., 2020. Micellar morphology of polysorbate 20 and 80 and their ester fractions in solution via small-angle neutron scattering. J. Pharm. Sci. 109 (4), 1498–1508. https://doi.org/10.1016/j.xphs.2019.12.016.

Penfield, K.W., Rumbelow, S., 2020. Challenges in polysorbate characterization by mass spectrometry. Rapid Commun. Mass Sp 34 (S2). https://doi.org/10.1002/rcm.8709.

Phaniendra, A., Jestadi, D.B., Periyasamy, L., 2015. Free radicals: properties, sources, targets, and their implication in various diseases. Indian J. Clin. Biochem. 30 (1), 11–26. https://doi.org/10.1007/s12291-014-0446-0.

Puschmann, J., Evers, D.-H., Müller-Goymann, C.C., Herbig, M.E., 2019. Development of a design of experiments optimized method for quantification of polysorbate 80 based on oleic acid using UHPLC-MS. J. Chromatogr. A 1599, 136–143. https://doi.org/10.1016/j.chroma.2019.04.015.

Qin, L., Huang, C.-H., Mao, L., Shao, B., Zhu, B.-Z., 2020. First unequivocal identification of the critical acyl radicals from the anti-tuberculosis drug isoniazid and its hydrazide analogs by complementary applications of ESR spin-trapping and HPLC/MS methods. Free Radic. Biol. Med. 154, 1–8. https://doi.org/10.1016/j.freeradbiomed.2020.04.021.

Rabe, M., Kerth, A., Blume, A., Garidel, P., 2020. Albumin displacement at the air–water interface by Tween (polysorbate) surfactants. Eur. Biophys. J. 49 (7), 533–547. https://doi.org/10.1007/s00249-020-01459-4.

Ravuri, K.S.K., 2018. Challenges in protein product development. Aaps Adv. Pharm. Sci. Ser. 25–62. https://doi.org/10.1007/978-3-319-90603-4_2.

Rodrigues, D., Tanenbaum, L.M., Thirumangalathu, R., Somani, S., Zhang, K., Kumar, V., Amin, K., Thakkar, S.V., 2021. Product-specific impact of viscosity modulating formulation excipients during ultra-high concentration biotherapeutics drug product development. J. Pharm. Sci. 110 (3), 1077–1082. https://doi.org/10.1016/j.xphs.2020.12.016.

Samouilov, A., Roubaud, V., Kuppusamy, P., Zweier, J.L., 2004. Kinetic analysis-based quantitation of free radical generation in EPR spin trapping. Anal. Biochem. 334 (1), 145–154. https://doi.org/10.1016/j.ab.2004.07.026.

Stoll, S., Schweiger, A., 2006. EasySpin, a comprehensive software package for spectral simulation and analysis in EPR. J. Magn. Reson. 178 (1), 42–55. https://doi.org/10.1016/j.jmr.2005.08.013.

Stolze, K., Udilova, N., Nohl, H., 2000. Spin trapping of lipid radicals with DEPMPO-derived spin traps: detection of superoxide, alkyl and alkoxyl radicals in aqueous and lipid phase. Free Rad. Bio. Med. 29 (10), 1005–1014. https://doi.org/10.1016/s0891-5849(00)00401-9.

Suzen, S., Gurer-Orhan, H., Saso, L., 2017. Detection of reactive oxygen and nitrogen species by electron paramagnetic resonance (EPR) technique. Molecules 22 (1), 181. https://doi.org/10.3390/molecules22010181.

Timmins, G.S., Liu, K.J., Bechara, E.J.H., Kotake, Y., Swartz, H.M., 1999. Trapping of free radicals with direct in vivo EPR detection: a comparison of 5,5-dimethyl-1-pyrroline-N-oxide and 5-diethoxyphosphoryl-5-methyl-1-pyrroline-N-oxide as spin traps for HO and SO4•−. Free Rad. Bio. Med. 27 (3–4), 329–333. https://doi.org/10.1016/s0891-5849(99)00049-0.

Tomlinson, A., Demeule, B., Lin, B., Yadav, S., 2015. Polysorbate 20 degradation in biopharmaceutical formulations: quantification of free fatty acids, characterization of particulates, and insights into the degradation mechanism. Mol. Pharm. 12 (11), 3805–3815. https://doi.org/10.1021/acs.molpharmaceut.5b00311.

Villamena, F.A., 2017. Reactive Species Detection in Biology, pp. 163–202. https://doi.org/10.1016/b978-0-12-420017-3.00004-9.

Villamena, F.A., Zweier, J.L., 2002. Superoxide radical trapping and spin adduct decay of 5-tert-butoxycarbonyl-5-methyl-1-pyrroline N-oxide (BocMPO): kinetics and theoretical analysis. J. Chem. Soc., Perkin Trans. 2 0 (7), 1340–1344. https://doi.org/10.1039/b201734b.

Wolff, S.P., 1994. [18] ferrous ion oxidation in presence of ferric ion indicator xylenol orange for measurement of hydroperoxides. Methods Enzymol. 233, 182–189. https://doi.org/10.1016/s0076-6879(94)33021-2.

Yang, R.-S., Bush, D.R., DeGraan-Weber, N., Barbacci, D., Zhang, L.-K., Letarte, S., Richardson, D., 2021. Advancing structure characterization of PS-80 by charge-reduced mass spectrometry and software-assisted composition analysis. J. Pharm. Sci. https://doi.org/10.1016/j.xphs.2021.08.036.

Yao, J., Dokuru, D.K., Noestheden, M., Park, S.S., Kerwin, B.A., Jona, J., Ostovic, D., Reid, D.L., 2009. A quantitative kinetic study of polysorbate autoxidation: the role of unsaturated fatty acid ester substituents. Pharm. Res. 26 (10), 2303–2313. https://doi.org/10.1007/s11095-009-9946-7.

Yin, H., Xu, L., Porter, N.A., 2011. Free radical lipid peroxidation: mechanisms and analysis. Chem. Rev. 111 (10), 5944–5972. https://doi.org/10.1021/cr200084z.

Zhang, L., Yadav, S., Demeule, B., Wang, Y.J., Mozziconacci, O., Schöneich, C., 2017. Degradation mechanisms of polysorbate 20 differentiated by 18O-labeling and mass spectrometry. Pharm. Res. 34 (1), 84–100. https://doi.org/10.1007/s11095-016-2041-y.

Zhang, S., Xiao, H., Li, N., 2021. Degradation of polysorbate 20 by sialate O-acetylesterase in monoclonal antibody formulations. J. Pharm. Sci. https://doi.org/10.1016/j.xphs.2021.09.001.